JOURNAL OF VIROLOGY, Feb. 2003, p. 1672–1681 Vol. 77, No. 3
0022-538X/03/$08.00+0 DOI: 10.1128/JVI.77.3.1672–1681.2003

Mouse Polyomavirus Utilizes Recycling Endosomes for a Traffic Pathway Independent of COPI Vesicle Transport

Petra Mannová and Jitka Forstová*

Department of Genetics and Microbiology, Charles University in Prague, 128 44 Prague 2, Czech Republic

Received 17 July 2002/Accepted 17 October 2002

Mouse polyomavirus enters host cells internalized, similar to simian virus 40 (SV40), in smooth monopinocytic vesicles, the movement of which is associated with transient actin disorganization. The major capsid protein (VP1) of the incoming polyomavirus accumulates on membranes around the cell nucleus. Here we show that unlike SV40, mouse polyomavirus infection is not substantially inhibited by brefeldin A, and colocalization of VP1 with β-COP during early stages of polyomavirus infection in mouse fibroblasts was observed only rarely. Thus, these viruses obviously use different traffic routes from the plasma membrane toward the cell nucleus. At approximately 3 h postinfection, a part of VP1 colocalized with the endoplasmic reticulum marker BiP, and a subpopulation of virus was found in perinuclear areas associated with Rab11 GTPase and colocalized with transferrin, a marker of recycling endosomes. Earlier postinfection, a minor subpopulation of virions was found to be associated with Rab5, known to be connected with early endosomes, but the cell entry of virus was slower than that of transferrin or cholera toxin B-fragment. Neither Rab7, a marker of late endosomes, nor LAMP-2 lysosomal glycoprotein was found to colocalize with polyomavirus. In situ hybridization with polyomavirus genome-specific fluorescent probes clearly demonstrated that, regardless of the multiplicity of infection, only a few virions delivered their genomic DNA into the cell nucleus, while the majority of viral genomes (and VP1) moved back from the proximity of the nucleus to the cytosol, apparently for their degradation.

Numerous animal viruses employ endocytic mechanisms for entry into the host cell. The most extensively studied endocytosis of viruses is that mediated by clathrin-coated pits (5, 7, 18, 20, 32). Individual members of the *Polyomaviridae* family apparently exploit different endocytic routes. Virions of these tumorigenic nonenveloped viruses contain the nucleocore (formed by genomic double-stranded DNA in complex with cellular histones and viral structural proteins) enclosed by the isometric capsid, 45 nm in diameter (6). The capsid is composed of 72 pentamers of the major structural protein, VP1. Two minor proteins, VP2 and VP3, form bridges which extend from the axial cavities of VP1 pentamers of the capsid shell into the nucleocore (4, 14).

The human polyomavirus JC recognizes the sialic acid moiety of its protein receptor and apparently enters glial cells by clathrin-dependent endocytosis (36). On the other hand, simian virus 40 (SV40), another member of the *Polyomaviridae*, binds to a major histocompatibility complex class I molecule on the surface of the host cell and enters cells in smooth monopinocytic vesicles containing caveolin-1 (2, 3, 29). SV40 infection is sensitive to cholesterol-sequestering drugs (1) and is also inhibited by a dominant negative mutant of caveolin (33, 41). Internalized SV40 virions were shown to enter larger, peripheral organelles, rich in caveolin-1, called caveosomes, and later were seen in tubular, caveolin-free membrane vesicles that moved along microtubules and delivered SV40 to the smooth endoplasmic reticulum (33). Recently, it has been reported that the transport of SV40 into the endoplasmic reticulum is brefeldin A sensitive and is mediated by intermediate compartments that contain β-COP, a component of COPI coatomer complexes employed in retrograde transport from the Golgi apparatus to the endoplasmic reticulum (30, 39).

Mouse polyomavirus is known to bind to the sialic acid residue of a not yet identified receptor (16, 45). It enters cells in tightly fitted monopinocytic vesicles, which are morphologically similar to those used by SV40 (13, 17, 19, 25). A strong inhibition of polyomavirus infection by methyl-β-cyclodextrin suggests an involvement of membrane raft domains in virus internalization (40). An induction of caveola formation in the areas of polyomavirus adsorption, fusions of polyomavirus-carrying vesicles with caveolin-rich vesicles and their movement from the membrane towards the cell nucleus accompanied by a transient disorganization of actin stress fibers resemble the transport described for SV40 (33, 34, 40). Colocalization of VP1 with microtubules in the later stages of polyomavirus movement and accumulation of VP1 around the cell nucleus observed in our laboratory (40) also suggest that polyomavirus and SV40 employ similar transport mechanisms. On the other hand, Gilbert and Benjamin observed little colocalization of polyomavirus with caveolin during viral entry and no effect of expression of a dominant-negative dynamin I mutant (required for the formation of both caveola-derived and clathrin-coated vesicles) on polyomavirus infection. This suggests that mouse polyomavirus might use a different class of vesicles for its trafficking (11).

Confocal microscopy has shown that at 3 h postinfection, VP1 of the incoming polyomavirus accumulates around the cell nucleus. However, neither free nor internalized viral particles that would account for the observed VP1 signal have

* Corresponding author. Mailing address: Department of Genetics and Microbiology, Charles University in Prague, Viničná 5, 128 44 Prague 2, Czech Republic. Phone: 420 2 21951730. Fax: 420 2 21951729. E-mail: jitkaf@natur.cuni.cz.

been revealed by electron microscopy (40). No VP1 signal has been detected inside the nucleus, suggesting either that only a few entire virions enter the cell nucleus (and are therefore below the detection level) and the vast majority of viral particles become disassembled and consequently degraded in the cytoplasm, or that virion uncoating can take place on cytoplasmic or nuclear membrane structures and the nuclear membrane is passed only by the viral nucleocores.

This study focuses on the following questions. (i) What is the character of membrane structures met by polyomavirus virions after their internalization? Is their transport towards the cell nucleus mediated, like that of SV40, by β-COP-containing vesicles? (ii) To what extent does the observed trafficking of viral particles represent cell defense mechanisms against viral infection? What proportion of virions successfully deliver their genomes into the nucleus?

MATERIALS AND METHODS

Cells and viruses. 3T6 Swiss albino mouse fibroblasts, normal murine mammary gland cells, and CV-1 monkey kidney epithelial cells were grown in Dulbecco's modified Eagle's medium (DMEM) supplemented with 10% fetal calf serum (FCS; Gibco) and 4 mM glutamine. Cells were cultivated at 37°C in a 5% CO_2 atmosphere. For virus propagation, 3T6 cells were infected with mouse polyomavirus, strain A2, at a multiplicity of infection of 0.1 PFU per cell. After 7 days, cells were harvested and virions were isolated by the procedure of Türler and Beard (47). SV40 was a kind gift of V. Vonka.

Immunofluorescence staining. 3T6 cells grown on glass coverslips were incubated with polyomavirus in DMEM (multiplicity of infection given for each experiment) for 1 h at 37°C. Virus was then removed, and DMEM with FCS was added. At the times postinfection indicated, the cells were washed three times with phosphate-buffered saline (PBS), fixed with 3% paraformaldehyde in PBS (30 min at room temperature), and permeabilized with 0.5% Triton X-100 in PBS (10 min).

For β-COP staining, the permeabilization step was performed with 0.5% Triton X-100–0.05% sodium dodecyl sulfate for 4 min. For LAMP-2 staining, cells were permeabilized with 0.05% saponin for 10 min. Fixed cells were washed with PBS and blocked with PBS–0.25% bovine serum albumin, 0.25% gelatin. Incubation with primary and secondary antibodies was carried out for 1.5 h and 0.5 h, respectively, with extensive washing with PBS after each incubation. VP1 was visualized with the mouse anti-VP1 polyclonal antibody (prepared in our laboratory), followed by the Alexa Fluor-594 (red) goat anti-mouse immunoglobulin antibody (Molecular Probes) or the Alexa Fluor-488 (green) rabbit anti-mouse immunoglobulin antibody (Molecular Probes). BiP (GRP78) and β-COP were stained with the rabbit anti-BiP or anti-β-COP purified antiserum (Alexis) followed by Alexa Fluor-488 (green) goat anti-rabbit immunoglobulin antibody (Molecular Probes).

Lamin A/C was visualized with the goat anti-lamin A/C polyclonal antibody (Santa Cruz Biotechnology) and the Alexa Fluor-546 (red) donkey anti-goat immunoglobulin antibody (Molecular Probes). Rab5 and Rab11 were stained with the respective rabbit antisera (kindly provided by J. Černý) and the Alexa Fluor-488 (green) goat anti-rabbit immunoglobulin antibody (Molecular Probes). Rab6 was visualized with the rabbit polyclonal antibody (Santa Cruz Biotechnology) and the Alexa Fluor-488 (green) goat anti-rabbit immunoglobulin antibody (Molecular Probes). Lysosome staining was performed with rat monoclonal anti-LAMP-2 antibody (Developmental Studies Hybridoma Bank, The University of Iowa, Iowa City) and the Alexa Fluor-488 (green) goat anti-rat immunoglobulin antibody (Molecular Probes). Transferrin-Alexa Fluor-488 (green; 50 μg/ml), kindly provided by J. Černý, and fluorescein isothiocyanate-labeled cholera toxin B-fragment (Sigma; 0.5 μg/ml) were used for colocalization studies. Colocalization with Rab7 was studied in 3T6 cells transfected with a recombinant plasmid carrying a gene for a Rab7-green fluorescent protein (GFP) fusion protein (provided by C. Bucci).

Fluorescence in situ hybridization. Linearized polyomavirus genomic DNA was used as a template for the preparation of the fluorescently labeled antipolyomavirus DNA probe. Incorporation of Chroma Tide Alexa Fluor-488–5-dUTP (Molecular Probes) by random primer labeling was performed according to the manufacturer's protocol; the resultant probe fragments appeared as a smear on 2% agarose gel electrophoresis, with the majority of fragments about 500 bp long. 3T6 cells grown on glass coverslips were fixed and permeabilized as described above. Cells were incubated with 0.1 M NaOH for 90 s and washed with 2× standard saline citrate buffer (2× SSC) twice for 40 s. Prehybridization buffer (3× SSC, 50% [vol/vol] formamide, 5× Denhardt's solution [27], denatured salmon sperm DNA to a concentration of 100 μg/ml) was added, and the samples were prehybridized for 1 h at 37°C. Subsequently, samples were sealed with a minimal volume of hybridization buffer (3× SSC, 50% [vol/vol] formamide, 5× Denhardt's solution, 10%[wt/vol] dextran sulfate, 100 μg of salmon sperm DNA per ml, 1 ng of labeled DNA probe per μl, denatured for 10 min at 95°C), incubated for 5 min at 85°C, and hybridized overnight at 45°C. Nonspecifically bound and excess probe was washed out by incubation with 3× SSC (three times for 5 min each at 37°C) and 0.5× SSC (twice for 5 min each at room temperature). Cells were rinsed with PBS and either mounted in 70% glycerol or further processed for indirect immunofluorescence staining of proteins as described above.

Confocal microscopy. Immunostained and in situ-hybridized cells were observed with a TNS SP Leica laser scanning confocal microscope. Sequential scanning of 0.5-μm sections was used for colocalization studies. Images were processed with TCS NT Leica software and Adobe Photoshop.

Brefeldin A experiment. 3T6 and CV-1 cells were incubated with polyomavirus and SV40, respectively, for 1 h at 4°C and then shifted to 37°C. At 0, 0.5, 1, 3, and 6 h at 37°C, virus was removed, and DMEM with FCS or DMEM with FCS and 0.5 μg of brefeldin A (Sigma) per ml was added, and cells were further incubated. Cells were fixed with methanol-acetone (1:1, vol/vol) for 3 min. Large T antigen of polyomavirus was detected with the rat anti-large T antigen 7 monoclonal antibody (9) and the Alexa Fluor-488 anti-rat immunoglobulin antibody (Molecular Probes). VP1 of polyomavirus was visualized as described above. The rabbit antiserum against SV40 VP1 and the mouse monoclonal anti-SV40 large T antigen antibody were kindly provided by H. Kasamatsu. Pictures were generated with an Olympus BX 60 fluorescence microscope equipped with a COHU high-performance charge-coupled device camera and processed with Lucia 32G software.

RESULTS

VP1 of incoming virions colocalizes with the endoplasmic reticulum marker BiP. Our previous studies revealed that mouse polyomavirus, like SV40, uses vesicles containing caveolin for its movement from the plasma membrane towards the cell nucleus. Electron microscopy showed that vesicles carrying viral particles fused with large membranous structures (40). To determine the character of these structures, the colocalization of VP1 with the endoplasmic reticulum-resident protein BiP (GRP78 [glucose-regulated protein 78]) was examined at 1, 3, and 6 h postinfection in infected 3T6 fibroblasts (Fig. 1). A significant colocalization was observed first at approximately 3 h postinfection. Six hours postinfection, the majority of VP1 apparently translocated from the endoplasmic reticulum into the cytosol, as only a few signals of colocalization of VP1 with BiP were observed.

Brefeldin A does not substantially inhibit mouse polyomavirus infection. Next, we addressed the question of whether the polyomavirus infection is affected by brefeldin A. This drug blocks the retrograde COPI-dependent transport between the Golgi complex and the endoplasmic reticulum by inhibiting guanine nucleotide exchange on the Arf1 GTPase that is essential for COPI coat assembly. We used SV40 infection for comparison. In agreement with the results of Norkin et al. (30) and Richards et al. (39), infection by SV40 was dramatically inhibited by brefeldin A treatment of cells. More than 90% inhibition of SV40 infection, measured by large T antigen appearance, was detected at 24 h postinfection (Fig. 2). Surprisingly, we did not observe any such effect of brefeldin A on polyomavirus infection. The decrease in the proportion of infected cells did not exceed 20%. This applied both to cells infected in the presence of brefeldin A (not shown) and for

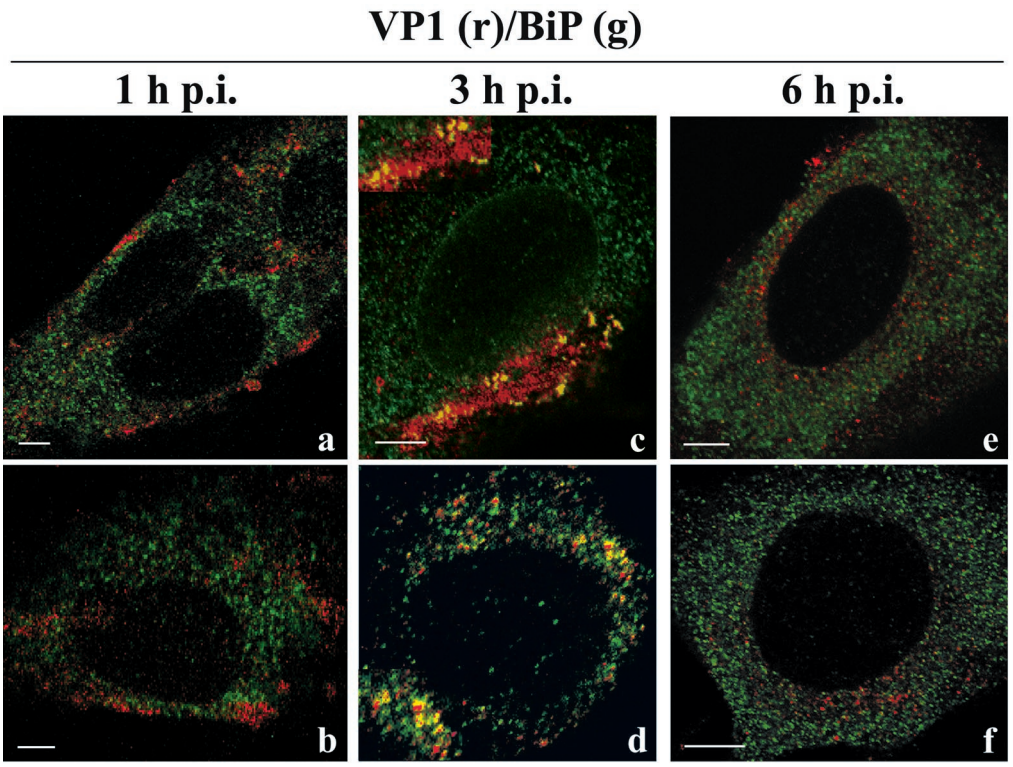

FIG. 1. Immunolocalization of VP1 (red) and BiP (green). 3T6 cells were infected with mouse polyomavirus (multiplicity of infection of 10^2 PFU per cell) and fixed at the times postinfection (p.i.) indicated (a and b, 1 h postinfection; c and d, 3 h postinfection; e and f, 6 h postinfection). Indirect immunofluorescence staining of VP1 (mouse polyclonal anti-VP1 antibody followed by Alexa Fluor-594 goat anti-mouse immunoglobulin) and the endoplasmic reticulum marker BiP (rabbit monoclonal anti-BiP antibody followed by Alexa Fluor-488 goat anti-rabbit immunoglobulin) was performed. Merged confocal sections are shown. Bars, 5 μm.

those to which brefeldin A was added at various times after their incubation with polyomavirus at 37°C (Fig. 2).

We did not observe any accumulating input polyomavirus virions in the intermediate compartment as described by Norkin et al. (30) for SV40 and as visible in Fig. 2A. We detected a lower intensity of polyomavirus large T antigen expression (but not a lower proportion of large T antigen-expressing cells) and significantly delayed appearance of VP1 expression in the brefeldin A-treated cells (24 h postinfection) in comparison with the nontreated ones, but we did not observe any substantial difference in VP1 production after prolonged incubation of cells in the presence of brefeldin A (44 h postinfection).

VP1 of polyomavirus virions colocalizes only rarely with the COPI marker β-COP. Colocalization of VP1 with β-COP, a coatomer protein of the COPI coat and a marker of the Golgi-endoplasmic reticulum intermediate compartment and COPI transport vesicles, was examined next (Fig. 3A). A substantial colocalization of SV40 and β-COP at the early stages of infection was observed recently (30). We found only a rare signal of colocalization of β-COP and polyomavirus VP1 during the interval from 10 min to 3 h postinfection. Moreover, in many cells, the VP1 signal appeared on the opposite side of β-COP-marked structures at 3 h postinfection (Fig. 3A).

Similar results were obtained both for infected mouse 3T6 fibroblasts (Fig. 3A) and normal murine mammary gland epithelial cells (not shown).

The results of both the brefeldin A inhibition experiments and β-COP colocalization experiments indicated that SV40 and mouse polyomavirus use different subclasses of vesicles for their trafficking towards the nucleus.

VP1 does not colocalize with Rab6 GTPase. To trace the endocytic traffic of polyomavirus to the endoplasmic reticulum, colocalization with different members of Rab family GTPases was examined. As COPI-coated vesicles are apparently not involved in polyomavirus transport, we examined the possibility of an alternative retrograde transport from Golgi to endoplasmic reticulum, like that used by Shiga toxin. This pathway is known to be connected with the Rab6 GTPase (48). However, no significant colocalization was detected (Fig. 3B).

Minor subpopulation of virions found associated with Rab5. We observed previously (40) that, like SV40, polyomavirus becomes internalized in smooth monopinocytic vesicles that fuse with larger vesicles which are mostly stainable with anti-caveolin antibody, presumably with caveosomes. Vesicles containing SV40 exhibited lack of the EEA1 marker of classical early endosomes (33). We used another marker of early endosomes, Rab5 GTPase (44), to examine its association with endosomes carrying polyomavirus. No massive colocalization of VP1 with Rab5 was observed in the early step of 3T6 fibroblast and normal murine mammary gland cell infection; nevertheless, clear association of a minor subpopulation of virus with Rab5 was identified (Fig. 4A).

It was observed (15) that transport from early endosomes is blocked at 20°C. Polyomavirus, when adsorbed and incubated

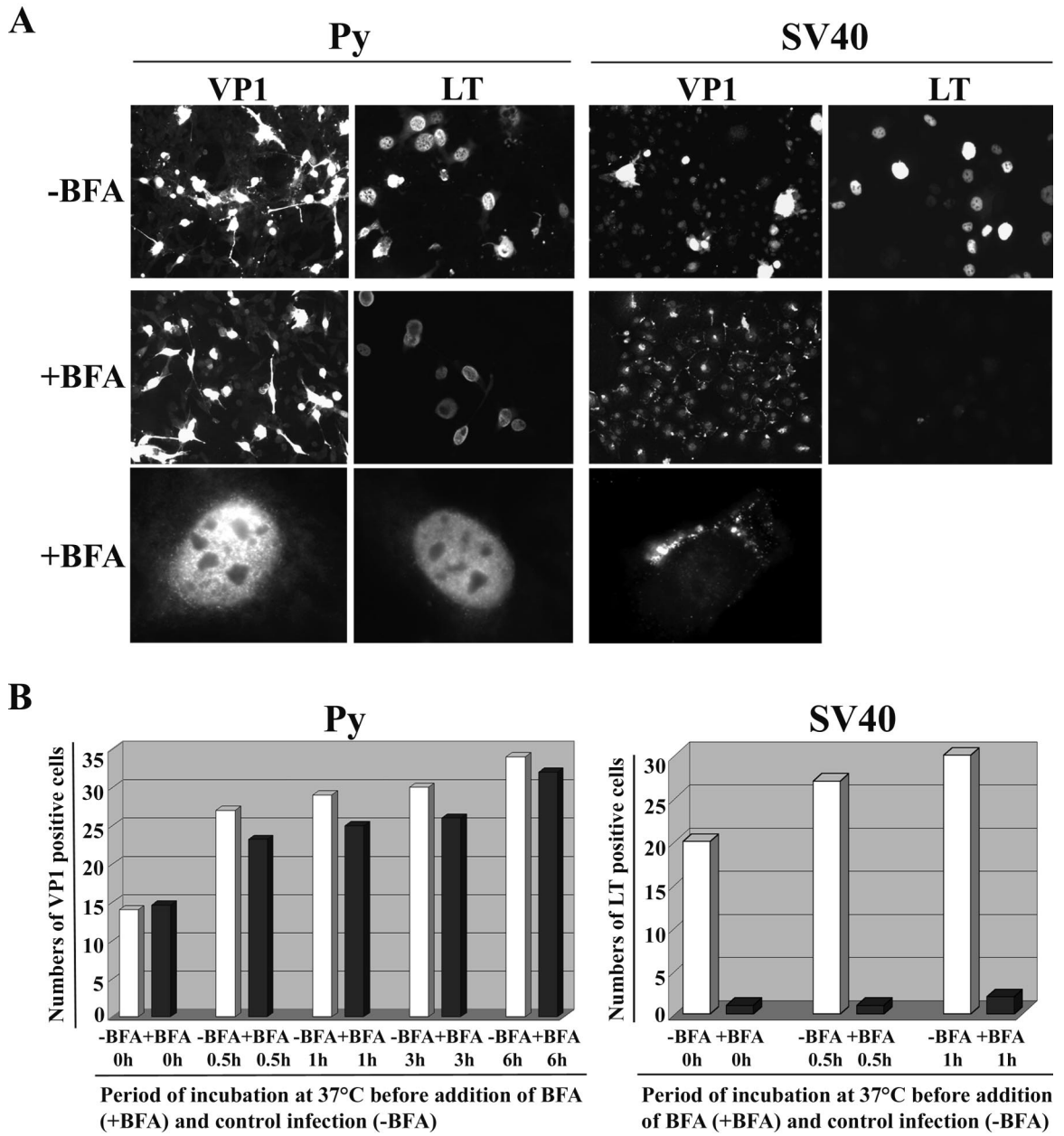

FIG. 2. Effect of brefeldin A treatment on polyomavirus and SV40 infection. (A) 3T6 cells were incubated with mouse polyomavirus (Py) (multiplicity of infection, 50 PFU per cell) for 1 h at 4°C and 0.5 h at 37°C. After that, FCS-containing medium without brefeldin A (−BFA) or with 0.5 μg of brefeldin A per ml (+BFA) was added, and cells were incubated until fixation (24 h postinfection for large T antigen (LT) and 44 h postinfection for VP1 immunodetection). CV-1 cells were infected with SV40 and treated with brefeldin A in the same manner as in the polyomavirus experiment, and cells were fixed at 24 h p.i and immunostained for large T antigen and VP1. Indirect immunofluorescence was done as described in the text. Photographs of representative microscopic fields are shown. (B) 3T6 or CV-1 cells were incubated with polyomavirus or SV40, respectively, for 1 h at 4°C. At 0, 0.5, 1, 3, or 6 h (for polyomavirus) after the shift to 37°C, medium containing FCS and 0.5 μg of brefeldin A per ml (+BFA) or without brefeldin A (−BFA) was added, and cells were further incubated. Cells were fixed at 44 h postinfection for immunostaining of VP1 or at 24 h postinfection for immunostaining of large T antigen. Positive cells were scored from 20 microscopic fields, and the averages are shown (standard deviations were lower than eight in all experiments).

for a 3-h interval at 20°C, mostly remained adsorbed to the cell surface. and part could be seen inside the cell in the periphery of the cytoplasm, not moving into perinuclear areas (Fig. 4B). No colocalization with cholera toxin B-fragment was found in the cytoplasm at 20°C, suggesting that internalized virus did not enter early endosomes at this temperature. However, little colocalization of virions with cholera toxin B-fragment was detected on the cell surface (Fig. 4B). Results similar to those with the cholera toxin B-fragment were also obtained with transferrin (Fig. 4B), which was described to accumulate in early and recycling endosomes in HeLa cells incubated at 20°C (26).

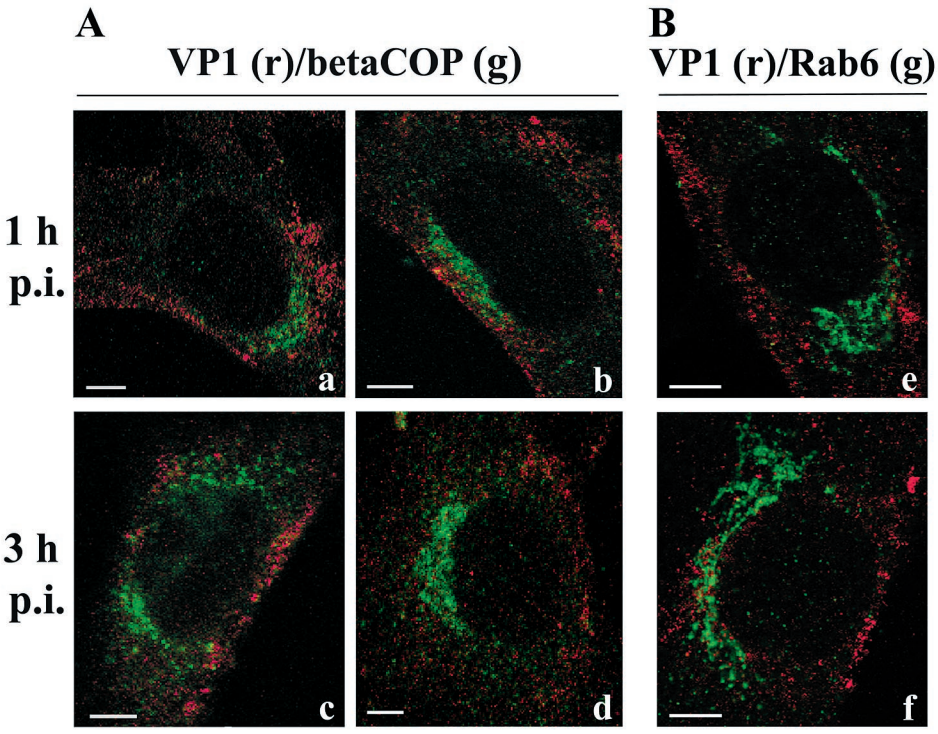

FIG. 3. Immunolocalization of VP1 (red) and β-COP (green) or VP1 (red) and Rab6 (green). 3T6 cells were infected with mouse polyomavirus (multiplicity of infection, 10^2 PFU per cell) and fixed at the times postinfection (p.i.) indicated (a, b, and e, 1 h postinfection; c, d, and f, 3 h postinfection). (A) Indirect immunofluorescence staining of VP1 (mouse polyclonal anti-VP1 antibody followed by Alexa Fluor-594 goat anti-mouse immunoglobulin) and COPI marker β-COP (rabbit monoclonal anti-β-COP antibody followed by Alexa Fluor-488 goat anti-rabbit immunoglobulin) was performed. (B) Staining of VP1 (mouse polyclonal anti-VP1 antibody followed by Alexa Fluor-594 goat anti-mouse immunoglobulin) and Rab6 GTPase (rabbit polyclonal anti-Rab6 antibody and Alexa Fluor-488 goat anti-rabbit immunoglobulin). Merged confocal sections are shown. Bars, 5 μm.

Substantial fraction of virus colocalizes with recycling endosome markers. Colocalization of VP1 with Rab11, a marker of perinuclear recycling endosomes (44), was observed at 3 h postinfection, when a substantial part of incoming virus reached the perinuclear area (Fig. 5A, b and c). Much less colocalization with Rab11 could be seen sooner (Fig. 5A, a). We further investigated whether transferrin, traveling from early to recycling endosomes, also meets the virus. A considerable part of the viral population clearly colocalized with transferrin at 3 h postinfection (Fig. 5B, e and f) although, to a small extent, some colocalizations were detected sooner (1 h postinfection; Fig. 5B, d).

Rab11 is assumed to be a sorting modulator at the exit of the recycling compartment, required for efficient transport from early endosomes via recycling endosomes to the trans-Golgi network (the pathway employed, e.g., by Shiga toxin). (26, 49) However, negative results of colocalization of virus with **c**holera toxin B-fragment**,** which accumulates at 37°C in the Golgi (not shown), as well as with β-COP and Rab6 markers suggested that polyomavirus probably bypasses the Golgi apparatus.

Neither late endosomes nor lysosomes are involved in mouse polyomavirus trafficking. Another route from recycling endosomes could be directed via late endosomes to lysosomes. Recently, canine parvovirus, which enters cells in clathrin-coated pits, was shown to use this pathway for delivery of its genomes into the cell nucleus (46). Confocal microscopy of the 3T6 cell line expressing the Rab7-GFP fusion protein did not reveal any connection of polyomavirus virions with this marker of late endosomes (43) at 1 or 3 h postinfection (Fig. 6A) or later postinfection (not shown). Also**,** double staining of cells with anti-LAMP-2 (lysosomal glycoprotein) and anti-VP1 antibodies proved the different locations of these proteins (Fig. 6B). Thus, the route of polyomavirus via late endosomes and lysosomes could be excluded.

Only a small proportion of virions deliver their genomic DNA to the cell nucleus. At about 3 h postinfection, we could see partial colocalization of VP1 with Rab11 and transferrin**,** which suggests that at least a subpopulation of virions appeared in recycling endosomes. At the same time, the marker for the endoplasmic reticulum, BiP, also colocalized in part with VP1. It has been reported that BiP, an endoplasmic reticulum lumenal chaperone**,** is involved in the export of abnormal proteins from the endoplasmic reticulum to the cytosol for their degradation (38). Considering this, we were interested to know the effectiveness of successful genome delivery by virions into the nucleus. Fluorescence microscopy analysis of cells double stained with antibodies against lamin A/C and against VP1 (3 h postinfection) revealed that the vast majority of the VP1 (if not all) remained spread around the nucleus. Only a few weak but distinct signals of VP1 on the lamina**,** which might represent VP1 of virions or nucleocores that crossed the

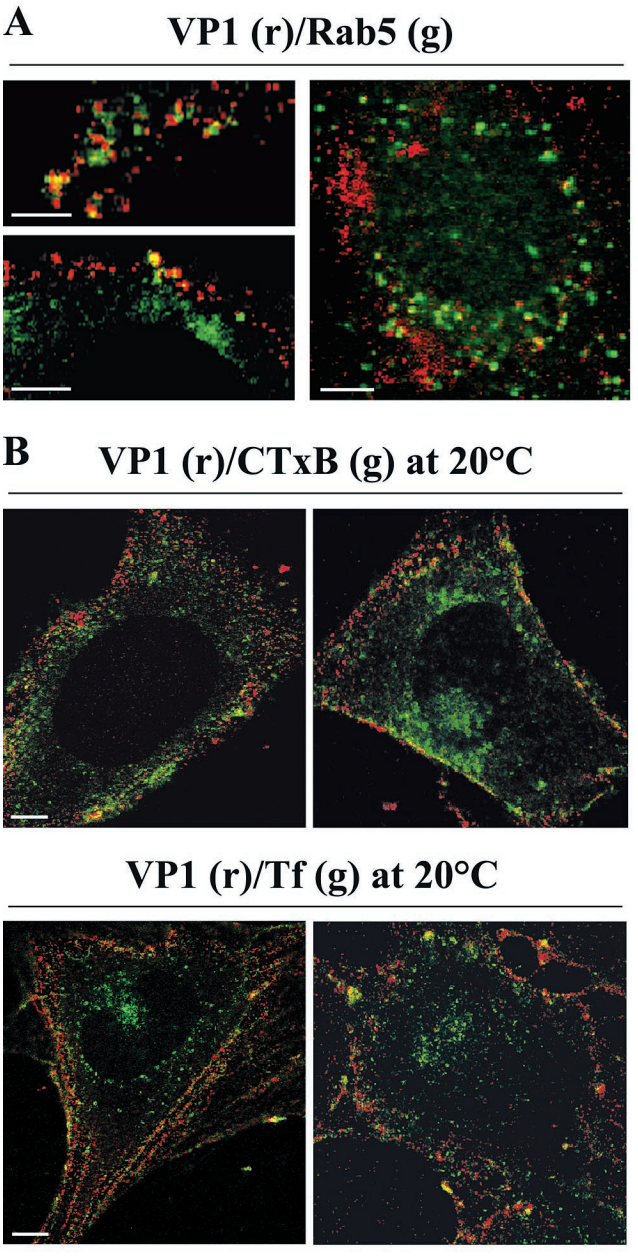

FIG. 4. (A) Immunolocalization of VP1 (red) and Rab5 (green). 3T6 cells were infected with mouse polyomavirus (multiplicity of infection, 10^2 PFU per cell) and fixed 1 h postinfection. Immunofluorescence staining of VP1 (mouse polyclonal anti-VP1 antibody followed by Alexa Fluor-594 goat anti-mouse immunoglobulin) and a marker of early endosomes, Rab5 GTPase (rabbit polyclonal anti-Rab5 antibody and Alexa Fluor-488 goat anti-rabbit immunoglobulin) was performed. Merged confocal sections are shown. Bars, 5 μm. (B) Colocalization study of VP1 (red) and CTxB (green) or Tf (green) at 20°C. 3T6 cells were incubated with mouse polyomavirus (multiplicity of infection, 10^2 PFU per cell) and fluorescein isothiocyanate-labeled cholera toxin B-fragment (CTxB, 0.5 μg/ml) or transferrin–Alexa Fluor-488 (Tf, 50 μg/ml) at 20°C for 3 h. Cells were fixed, and VP1 was visualized by immunostaining (mouse polyclonal anti-VP1 antibody followed by Alexa Fluor-594 goat anti-mouse immunoglobulin). Merged confocal sections are shown. Bars, 5 μm.

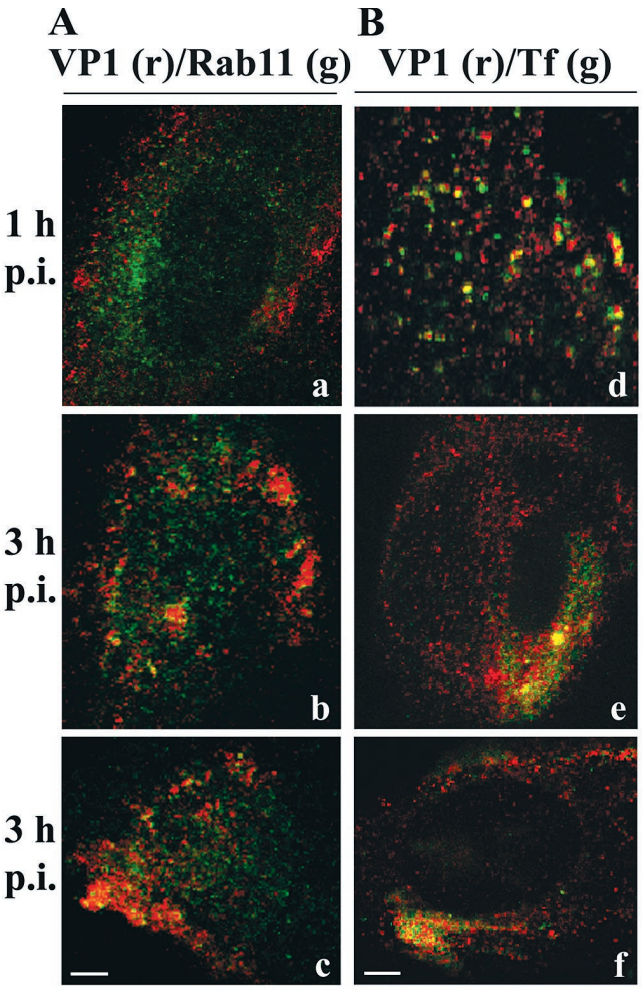

FIG. 5. (A) Immunolocalization of VP1 (red) and Rab11 (green). 3T6 cells were infected with mouse polyomavirus (multiplicity of infection, 10^2 PFU per cell) and fixed 1 h postinfection (a) or 3 h postinfection (b and c). Immunofluorescence staining of VP1 (mouse polyclonal anti-VP1 antibody followed by Alexa Fluor-594 goat anti-mouse immunoglobulin) and a marker of recycling endosomes, Rab11 GTPase (rabbit polyclonal anti-Rab11 antibody and Alexa Fluor-488 goat anti-rabbit immunoglobulin), was performed. Merged confocal sections are shown. Bars, 5 μm. (B) Colocalization study of VP1 (red) and transferrin (green). 3T6 cells were incubated with mouse polyomavirus (multiplicity of infection, 10^2 PFU per cell) and transferrin-Alexa Fluor-488 (Tf, 50 μg/ml) for 1 h (d) or 3 h (e and f) at 37°C. Cells were fixed, and VP1 was visualized by immunostaining (mouse polyclonal anti-VP1 antibody followed by Alexa Fluor-594 goat anti-mouse immunoglobulin). Merged confocal sections are shown. Bars, 5 μm.

membrane, were noticed (Fig. 7A). However, their precise location towards the nuclear membrane remains to be determined.

In order to follow the fate of the genomes of incoming virions, we applied the in situ DNA hybridization technique combined with confocal fluorescence microscopy. In situ hybridization of infected cells with polyomavirus genome-specific fluorescent probes clearly demonstrated not only that the majority of VP1 did not enter cell nuclei (when a multiplicity of infection of 100 PFU and more was used) but that this applied to the majority of viral genomes as well (Fig. 7B).

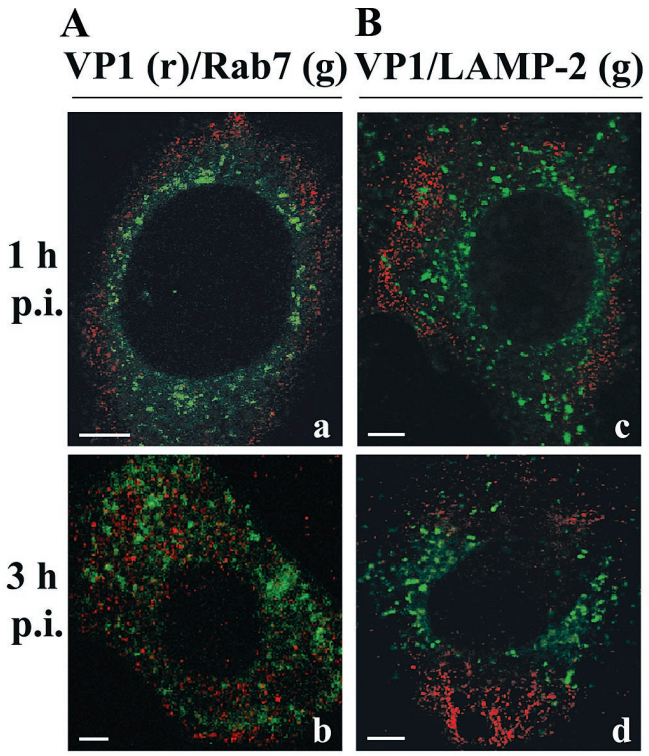

FIG. 6. (A) Colocalization study of VP1 (red) and Rab7-GFP. The 3T6 cell line expressing the Rab7-GFP fusion protein was infected with mouse polyomavirus (multiplicity of infection, 10^2 PFU per cell). Cells were fixed at 1 h (a) or 3 h (b) postinfection (p.i.), and VP1 was immunostained with mouse polyclonal anti-VP1 antibody followed by Alexa Fluor-594 goat anti-mouse immunoglobulin. Merged confocal sections are shown. Bars, 5 μm. (B) Immunolocalization of VP1 (red) and LAMP-2 (green). 3T6 cells were infected with mouse polyomavirus (multiplicity of infection, 10^2 PFU per cell) and fixed at 1 h postinfection (c) or 3 h postinfection (d). Immunofluorescence staining of VP1 (mouse polyclonal anti-VP1 antibody followed by Alexa Fluor-594 goat anti-mouse immunoglobulin) and LAMP-2, a marker protein of lysosomes (rat monoclonal anti-LAMP-2 antibody and Alexa Fluor-488 goat anti-rat immunoglobulin) was performed. Merged confocal sections are shown. Bars, 5 μm.

The polyomavirus genomes inside the nucleus could first be detected at 6 h postinfection, when a few very weak green dots of the DNA hybridization signal appeared in the interior of the nucleus (besides a strong signal in the cytoplasm caused by those polyomavirus genomes that failed to reach the cell nucleus). Later postinfection (10 and 15 h), the points of the hybridization signal became more apparent as the replication of virus genomes proceeded. We have never detected such signals in control, mock-infected cells. (Fig. 7B) The strong DNA signal, which remained in the cytoplasm at 3 and 6 h postinfection, disappeared after several further hours.

DISCUSSION

Previous electron and confocal microscopy studies have revealed that internalization and intracellular transport of mouse polyomavirus and SV40 display several common features: both viruses are prevalently internalized into smooth monopinocytic vesicles that can fuse with caveolin-1-rich endosomes. Both simian and mouse polyomaviruses seem to use the actin and tubulin cytoskeleton for their movements, and their infections are sensitive to methyl-β-cyclodextrin (13, 17, 19, 25, 34, 40).

Despite the observed similarities, we revealed a crucial difference in the movement of both viruses: only rare colocalization of the COPI marker β-COP with polyomavirus virions was observed in 3T6 fibroblasts (Fig. 3A) as well as in normal murine mammary gland epithelial cells (not shown), while extensive colocalization was reported for SV40 VP1 at 3 and 5 h postinfection (30). Moreover, brefeldin A displayed substantially different effects on the infection efficiencies of the two viruses. While SV40 infection was inhibited dramatically by this drug (30, 39) (Fig. 2), that of polyomavirus was delayed when followed for 24 h postinfection and only slightly affected (measured by the number of cells positive for late viral expression) after 44 h of incubation in the presence of the drug. These data suggest that these viruses use different vesicles for their movement toward the cell nucleus.

SV40 uses a COPI-mediated retrograde transport pathway to the endoplasmic reticulum similar to that of cholera toxin, which also uses caveolae for its internalization (22, 23, 31). It was found that COPI plays a critical role in the appearance of the endoplasmic reticulum-Golgi intermediate compartment, which is composed of clusters of vesicles and small tubules (35). Pelkmans et al. described a two-stage pathway of SV40 trafficking: the monopinocytic vesicles containing SV40, with the help of actin tails, first fuse with caveosomes, large peripheral organelles, where SV40 is sorted into tubular, caveolin-free membrane vesicles that move rapidly along microtubules toward the endoplasmic reticulum (33, 34). A similar tubular membrane network containing SV40 virions was also observed by Kartenbeck et al. (19). We have never detected such tubular, caveolin-free membrane structures in the polyomavirus-infected cells, but caveolin-1 seemed to accompany at least a subpopulation of incoming polyomaviruses into perinuclear areas (40).

Surprisingly, our confocal studies with markers of different endocytic compartments strongly suggested the association of polyomavirus with recycling endosomes. At approximately 3 h postinfection, when VP1 appeared closer to the cell nucleus, considerable colocalization of VP1 with the recycling endosome marker Rab11 was detected. At the same time, a similar extent of colocalization was observed with transferrin when both transferrin and virus were added to cells at 37°C.

The observed occasional colocalization of Rab5 and VP1 could also reflect a connection of virions with early endosomes. However, when transferrin and virus were adsorbed at 0°C and then shifted for 30 to 60 min to 37°C, little or no colocalization of VP1 and transferrin was observed. Colocalization with Rab5 was also sporadic. The explanation could be that internalization and movement of virus was slowed down, e.g., by disturbed cytoskeleton structures, and transferrin, internalized in clathrin-coated vesicles, overtook the virus and was already localized in recycling endosomes. Moreover, the kinetics of polyomavirus uptake is slower than the internalization of viruses utilizing clathrin-coated pits (25, 32; our unpublished results), and the transit of transferrin through early endosomes was found to be extremely rapid (50).

However, the sporadic colocalization of Rab5 and VP1 could reflect the possibility that monopinocytic vesicles and

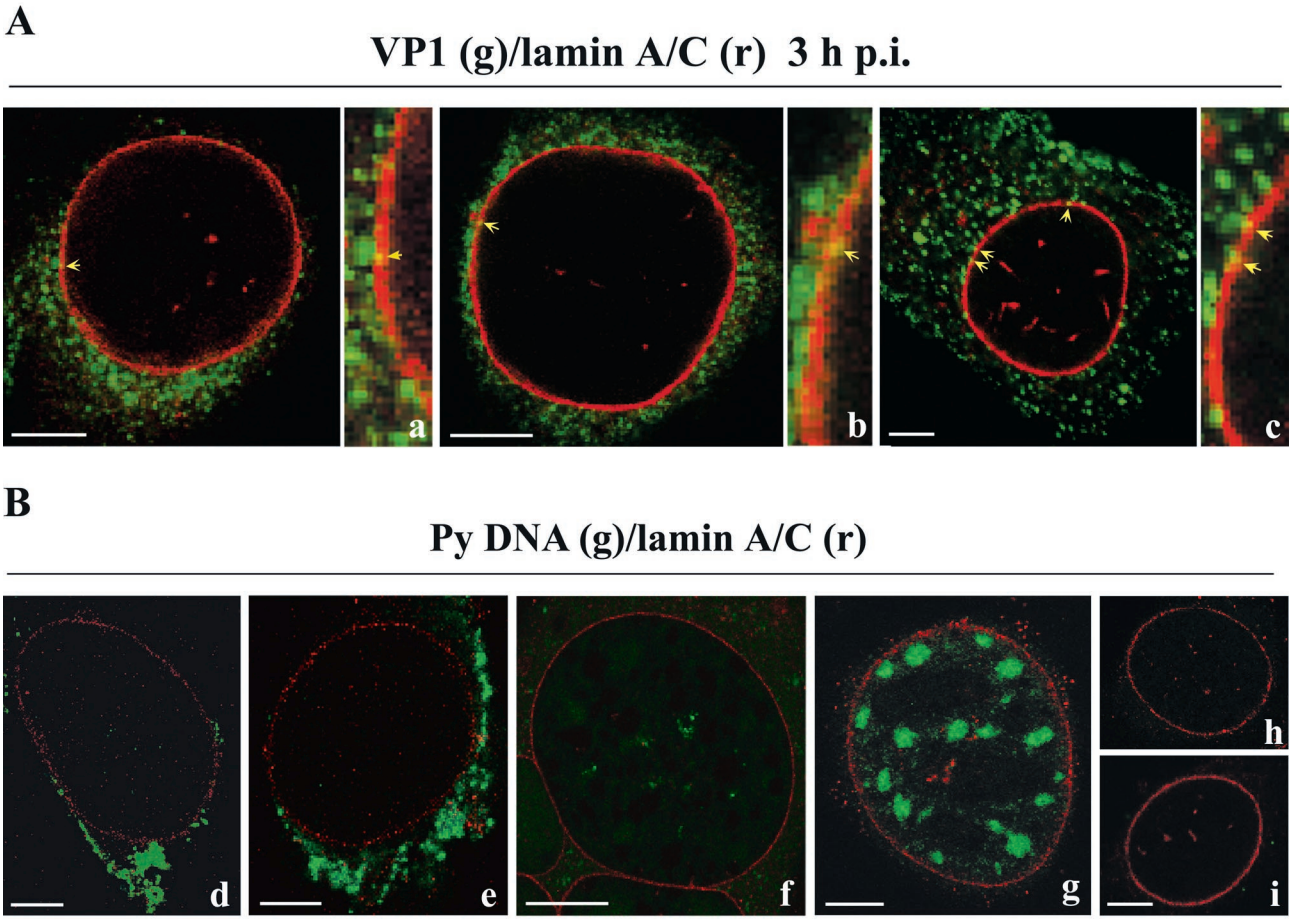

FIG. 7. (A) Immunolocalization of VP1 (green) and lamin A/C (red). 3T6 cells were infected with mouse polyomavirus ([a and b] multiplicity of infection, 5×10^2 PFU per cell; [c] multiplicity of infection, 10^2 PFU per cell) and fixed at 3 h postinfection. Indirect immunofluorescent staining of VP1 (mouse polyclonal anti-VP1 antibody followed by Alexa Fluor-488 rabbit anti-mouse immunoglobulin) and lamin A/C (goat polyclonal anti-lamin A/C antibody followed by Alexa Fluor-546 donkey anti-goat immunoglobulin) was performed, and merged confocal sections are shown. Bars, 5 μm. (B) Localization of polyomavirus DNA (green) and lamin A/C (red). 3T6 cells were infected with mouse polyomavirus (Py) ([d and e] multiplicity of infection, 5×10^2 PFU per cell; [f and g] multiplicity of infection, 10^2 PFU per cell). Cells were fixed at 6 h postinfection (d and e), 10 h postinfection (f), or 15 h postinfection (g), and polyomavirus DNA was detected by in situ hybridization with the Alexa Fluor-488–5-dUTP-stained random-primed probes against the polyomavirus genome (see text). Indirect immunofluorescence staining of lamin A/C (goat polyclonal anti-lamin A/C antibody followed by Alexa Fluor-546 donkey anti-goat immunoglobulin) was performed after in situ hybridization. Merged confocal sections are shown. As a negative control, in situ hybridization and immunostaining of lamin A/C on noninfected 3T6 cells were done (h and i). Bars, 5 μm.

larger caveolin-1-rich vesicles carrying viral particles fuse predominantly with recycling endosomes, mostly bypassing early endosomes. While the EEA1 endosomal marker (Rab5 effector protein) is restricted to early endosomes, Rab5 GTPase can also be detected in recycling endosomes, although at low abundance. It agrees with the observations that this GTPase is able to function through more than one effector (44). The experiment of adsorption and incubation of virus at 20°C, a temperature at which the cargo is trapped in early endosomes, showed (i) considerable inhibition of virion internalization, (ii) block of movement of the internalized virion minority from the periphery of the cytoplasm, and (iii) no viral association with early endosomes inside the cell as partial colocalization with Rab5 (not shown), cholera toxin B-fragment, or transferrin could be seen only on the plasma membrane. Sensitivity of SV40 internalization to 20°C was also noticed (39). However, no staining of SV40 was found either on the surface of or inside the cells infected at 20°C, suggesting even inefficient surface binding.

Gagescu et al. (10) isolated and investigated recycling endosomes in Madin-Darby canine kidney cells and found a high content of lipids (cholesterol and sphingomyelin) and proteins (e.g., flotillin-1 or caveolin-1) associated in plasma membrane rafts. Moreover, glycosylphosphatidyl inositol-anchored proteins, which are also associated with rafts on the cell surface, were found to follow the same pathway as transferrin receptor after endocytosis into nonpolarized cells, albeit with slower kinetics (28). All those findings fit with our previous observations of the presence of the caveolin-1 label on monopinocytic vesicles carrying polyomavirus virions and the fact that caveolin staining accompanied VP1 from the plasma membrane to the perinuclear areas (40).

One of the questions remaining to be answered is the further

route of virions from recycling endosomes. The pathway from recycling endosomes to late endosomes and lysosomes recently described for canine parvovirus (46) is not used by mouse polyomavirus, as colocalization with neither the Rab7 GTPase nor the LAMP-2 lysosomal glycoprotein has been detected. Another route, employed by, e.g., Shiga toxin, leads from the recycling endosomes to the Golgi apparatus (26). From the Golgi apparatus, COPI-independent and brefeldin A-insensitive retrograde transport to the endoplasmic reticulum was described for this toxin (12, 48). To investigate whether polyomavirus exploits this pathway, we examined colocalization with Rab6, a Golgi-associated GTPase, accompanying Shiga toxin B-fragment during retrograde transport from the Golgi to the endoplasmic reticulum (48). However, no convincing Rab6 association with the polyomavirus transport system was found. Cholera toxin B-fragment, which is known to accumulate in the Golgi (21), did not colocalize with VP1 either (not shown). Thus, the Golgi apparatus seems to be bypassed by mouse polyomavirus, and the route of the virus from recycling endosomes to the endoplasmic reticulum remains unclear. The observed delay of polyomavirus infection in the presence of brefeldin A might account for the role of recycling endosomes in productive infection and could be explained by a sorting delay due to an altered endosome morphology caused by brefeldin A (24).

Another possibility, the direct transport of a subpopulation of polyomavirus in monopinocytic (or/and larger, fused) vesicles from the plasma membrane to the endoplasmic reticulum, cannot be ruled out either. Several direct fusions of monopinocytic vesicles carrying virus particles with the endoplasmic reticulum detected by electron microscopy of cell sections (40) account for this possibility. Smart et al. studied the movement of caveolin in response to cholesterol oxidation and found that it moves first from caveolae into the endoplasmic reticulum and thereafter to the Golgi apparatus. Brefeldin A did not prevent the initial movement of caveolin from the plasma membrane into the cell, but did prevent it from reaching the Golgi apparatus (42).

An endocytic route targeted into the endoplasmic reticulum might also play a role in the cell defense against invading pathogens. Eukaryotic cells possess a complex degradation machinery that eliminates misfolded, unassembled proteins from the endoplasmic reticulum. These degradation mechanisms require retrograde translocation of proteins from the endoplasmic reticulum back to the cytosol. It has been reported that BiP, an endoplasmic lumenal chaperone (which colocalized at 3 h postinfection with polyomavirus VP1) is involved in the export of abnormal proteins from the endoplasmic reticulum to the cytosol (38).

Following the possibility that the observed trafficking of polyomavirus is a part of the cell defense mechanisms, we examined the effectiveness of successful genome delivery by virions into the nucleus. In situ hybridization of viral genomes with fluorescently labeled polyomavirus DNA proved that, indeed, the majority of virions observed traveled to their destruction. Their trafficking may represent an endocytic process leading to the endoplasmic reticulum-associated protein degradation pathway (37). Several protein toxins, including the A chain of ricin, enter mammalian cells by endocytosis and subsequently reach their cytosolic substrates by translocation across the endoplasmic reticulum membrane. Such toxins exploit the endoplasmic reticulum-associated protein degradation pathway but must escape (at least in part) the normal fate of endoplasmic reticulum-associated degradation pathway substrates, i.e., degradation (8).

It is possible that mouse polyomavirus uses this mechanism, too. If that is the case, the translocation of viral particles across the endoplasmic reticulum membrane into the cytosol and their partial proteolysis by the endoplasmic reticulum-associated degradation pathway might help to release nucleocores, a minor fraction of which escape into the nucleus before it would be degraded. Thus, the polyomavirus might misuse the pathway destined by cells for its destruction. However, the possibility that successful virions and those targeted to degradation use different trafficking routes cannot be excluded. The fate of virions may be decided already during their internalization, and the protein composition of raft structures delivering virions into recycling endosomes might play a role in their sorting.

ACKNOWLEDGMENTS

This work was generously supported in part by the HHMI USA (grant 75195-540501), by the Grant Agency of the Czech Republic (grant 204/00/0271), and by the Ministry of Education of the Czech Republic (MSM 113100003).

We are grateful to H. Kasamatsu, J. Černý, and L. Turek for gifts of antibodies, to V. Vonka for SV40, and to D. Holá and Ŝ. Takáčová for assistance in preparation of the manuscript.

REFERENCES

1. **Anderson, H. A., Y. Chen, and L. C. Norkin.** 1996. Bound simian virus 40 translocates to caveolin-enriched membrane domains, and its entry is inhibited by drugs that selectively disrupt caveolae. Mol. Biol. Cell **11:**1825–1834.
2. **Anderson, H. A., Y. Chen, and L. C. Norkin.** 1998. Major histocompatibility complex class I molecules are enriched in caveolae but do not enter with simian virus 40. J. Gen. Virol. **79:**1469–1477.
3. **Atwood, W. J., and L. C. Norkin.** 1989. Class I major histocompatibility proteins as cell surface receptors for simian virus 40. J. Virol. **63:**4474–4477.
4. **Barouch, D. H., and S. C. Harrison.** 1994. Interactions among the major and minor coat proteins of polyomavirus. J. Virol. **68:**3982–3989.
5. **Bartlett, J. S., R. Wilcher, and R. J. Samulski.** 2000. Infectious entry pathway of adeno-associated virus and adeno-associated virus vectors. J. Virol. **74:** 2777–2785.
6. **Brady, J. N., V. D. Winston, and R. A. Consigli.** 1978. Characterization of DNA polyomavirus by treatment with ethylene glycol-bis-*N*,*N*′-tetraacetic acid and dithiothreitol. J. Virol. **27:**193–204.
7. **Chardonnet, Y., and S. Dales.** 1970. Early events in the interaction of adenoviruses with HeLa cells. I. Penetration of type 5 and intracellular release of the DNA genome. Virology **40:**462–477.
8. **Deeks, E. D., J. P. Cook, P. J. Day, D. C. Smith, L. M. Roberts, and J. M. Lord.** 2002. The low lysine content of ricin A chain reduces the risk of proteolytic degradation after translocation from the endoplasmic reticulum to the cytosol. Biochemistry **41:**3405–3413.
9. **Dilworth, S. M., and B. E. Griffin.** 1982. Monoclonal antibodies against polyomavirus virus tumor antigens. Proc. Natl. Acad. Sci. USA **79:**1059–1063.
10. **Gagescu, R., N. Demaurex, R. G. Parton, W. Hunziker, L. A. Huber, and J. Gruenberg.** 2000. The recycling endosome of Madin-Darby canine kidney cells is a mildly acidic compartment rich in raft components. Mol. Biol. Cell **11:**2775–2791.
11. **Gilbert, J. M., and T. L. Benjamin.** 2000. Early steps of polyomavirus entry into cells. J. Virol. **74:**8582–8588.
12. **Girod, A., B. Storrie, J. C. Simpson, L. Johannes, B. Goud, L. M. Roberts, J. M. Lord, T. Nilsson, and R. Pepperkok.** 1999. Evidence for a COPI-independent transport route from the Golgi complex to the endoplasmic reticulum. Nat. Cell Biol. **1:**423–430.
13. **Griffith, G. R., and R. A. Consigli.** 1984. Isolation and characterization of monopinocytotic vesicles containing polyomavirus from the cytoplasm of infected mouse kidney cells. J. Virol. **50:**77–85.
14. **Griffith, J. P., D. L. Griffith, I. Rayment, W. T. Murakami, and D. L. D. Caspar.** 1992. Inside polyomavirus at 25 Å resolution. Nature **355:**625–654.
15. **Griffiths, G., B. Hoflack, K. Simons, I., Mellman, and S. Kornfeld.** 1988. The mannose 6-phosphate receptor and the biogenesis of lysosomes. Cell **52:**329–341.

16. **Haun, G., O. T. Keppler, C. T. Bock, M. Herrmann, H. Zentgraf, and M. Pawlita.** 1993. The cell surface receptor is a major determinant restricting the host range of the B-lymphotropic papovavirus. J. Virol. **67:**7482–7492.
17. **Hummeler, K., N. Tomassini, and F. Sokol.** 1970. Morphological aspect of the uptake of simian virus 40 by permissive cells. J. Virol. **6:**87–93.
18. **Joki-Korpela, P., V. Marjomaki, C. Krogerus, J. Heino, and T. Hyypia.** 2001. Entry of human parechovirus 1. J. Virol. **75:**1958–1967.
19. **Kartenbeck, J., H. Stukenbrok, and A. Helenius.** 1989. Endocytosis of simian virus 40 into the endoplasmic reticulum. J. Cell Biol. **109:**2721–2729.
20. **Krizanova, O., F. Ciampor, and P. Verber.** 1982. Influence of chlorpromazine on the replication of influenza virus in chick embryo fibroblasts. Acta Virol. **26:**209–216.
21. **Lencer, W. I.** 2001. Microbes, and microbial toxins. Paradigms for microbial-mucosal toxins. V. Cholera: invasion of the intestinal epithelial barrier by a stably folded protein toxin. Am. J. Physiol. Gastrointest. Liver Physiol. **280:** G781–G786.
22. **Lencer, W. I., C. Constable, S. Moe, M. G. Jobling, H. M. Webb, S. Ruston, J. L. Madara, T. R. Hirst, and R. K. Holmes.** 1995. Targeting of cholera toxin and *Escherichia coli* heat-labile toxin in polarized epithelia: role of COOH-terminal KDEL. J. Cell Biol. **131:**951–962.
23. **Lencer, W. I., T. R. Hirst, and R. K. Holmes.** 1999. Membrane traffic and the cellular uptake of cholera toxin. Biochim. Biophys. Acta **1450:**177–190.
24. **Lippincott-Schwartz, J., L. Yuan, C. Tipper, M. Amherdt, L. Orci, and R. D. Klausner.** 1991. Brefeldin A's effects on endosomes, lysosomes, and the TGN suggest a general mechanism for regulating organelle structure and membrane traffic. Cell **67:**601–616.
25. **Mackay, R. L., and R. A. Consigli.** 1976. Early events in polyomavirus virus infection: attachment, penetration, and nuclear entry. J. Virol. **19:**620–636.
26. **Mallard, F., C. Antony, D. Tenza, J. Salamero, B. Goud, and L. Johannes.** 1998. Direct pathway from early/recycling endosomes to the Golgi apparatus revealed through the study of Shiga toxin B-fragment transport. J. Cell Biol. **143:**973–990.
27. **Maniatis, T., E. F. Fritsch, and J. Sambrook.** 1982. Molecular cloning: a laboratory manual. Cold Spring Harbor Laboratory Press, Cold Spring Harbor, N.Y.
28. **Mayor, S., S. Sabharanjak, and F. R. Maxfield.** 1998. Cholesterol-dependent retention of GPI-anchored proteins in endosomes. EMBO J. **17:**4626–4638.
29. **Norkin, L. C.** 1999. Simian virus 40 infection via major histocompatibility complex class I molecules and caveolae. Immunol. Rev. **168:**13–22.
30. **Norkin, L. C., H. A. Anderson, W. A. Scott, and A. Oppenheim.** 2002. Caveolar endocytosis of simian virus 40 is followed by brefeldin A-sensitive transport to the endoplasmic reticulum, where the virus disassembles. J. Virol. **76:**5156–5166.
31. **Orlandi, P. A., and P. H. Fishman.** 1998. Filipin-dependent inhibition of cholera toxin: evidence for toxin internalisation and activation through caveolae-like domains. J. Cell Biol. **141:**905–915.
32. **Parker, J. S., and C. R. Parrish.** 1999. Cellular uptake and infection by canine parvovirus involves dynamin-regulated clathrin-mediated endocytosis, followed by slower intracellular trafficking. J. Virol. **74:**1919–1930.
33. **Pelkmans, L., J. Kartenbeck, and A. Helenius.** 2001. Caveolar endocytosis of simian virus 40 reveals a new two step vesicular-transport pathway to the endoplasmic reticulum. Nat. Cell Biol. **3:**473–483.
34. **Pelkmans, L., D. Püntener, and A. Helenius.** 2002. Local actin polymerization and dynamin recruitment in SV40-induced internalization of caveolae. Science **296:**535–539.
35. **Peter, F., H. Plutner, H. Zhu, T. E. Kreis, and W. E. Balch.** 1993. Beta-COP is essential for transport of protein from the endoplasmic reticulum to the Golgi in vitro. J. Cell Biol. **122:**1155–1167.
36. **Pho, M. T., A. Ashok, and W. J. Atwood.** 2000. JC virus enters human glial cells by clathrin-dependent receptor-mediated endocytosis. J. Virol. **74:**2288–2292.
37. **Plemper, R. K., and D. H. Wolf.** 1999. Retrograde protein translocation: ERADication of secretory proteins in health and disease. Trends Biochem. Sci. **24:**266–270.
38. **Plemper, R. K., S. Bohmler, J. Bordallo, T. Sommer, and D. H. Wolf.** 1997. Mutant analysis links the translocon and BiP to retrograde protein transport for endoplasmic reticulum degradation. Nature **388:**891–895.
39. **Richards, A. A., E. Stang, R. Pepperkok, and R. G. Parton.** 2002. Inhibitors of COP-mediated transport and cholera toxin action inhibit simian virus 40 infection. Mol. Biol. Cell **13:**1750–1764.
40. **Richterová, Z., D. Liebl, M. Horák, Z. Palková, J. Štokrová, P. Hozák, J. Korb, and J. Forstová.** 2001. Caveolae are involved in the trafficking of mouse polyomavirus virions and artificial VP1 pseudocapsids toward cell nuclei. J. Virol. **75:**10880–10891.
41. **Roy, S., R. Luetterforst, A. Harding, A. Apolloni, M. Etheridge, E. Stang, B. Rolls, J. F. Hancock, and R. G. Parton.** 1999. Dominant-negative caveolin inhibits H-Ras function by disrupting cholesterol-rich plasma membrane domains. Nat. Cell Biol. **2:**98–105.
42. **Smart, E. J., Y. Yun-Shu, P. A. Conrad, and R. G. W. Anderson.** 1994. Caveolin moves from caveolae to the Golgi apparatus in response to cholesterol oxidation. J. Cell Biol. **127:**1185–1197.
43. **Somsel Rodman, J., and A. Wandinger-Ness.** 2000. Rab GTPases coordinate endocytosis. J. Cell Sci. **113:**183–192.
44. **Sönnichsen, B., S. De Renzis, E. Nielsen, J. Rietdorf, and M. Zerial.** 2000. Distinct membrane domains on endosomes in the recycling pathway visualized by multicolor imaging of Rab4, Rab5, and Rab11. J. Cell Biol. **149:**901–913.
45. **Stehle, T., and S. C. Harrison.** 1996. Crystal structures of murine polyomavirus in complex with straight-chain and branched-chain sialyloligosaccharide receptor fragments. Structure **4:**183–194.
46. **Suikkanen, S., K. Sääjärvi, J. Hirsimäki, O. Välilehto, H. Reunanen, M. Vihinen-Ranta, and M. Vuento.** 2002. Role of recycling endosomes and lysosomes in dynein-dependent entry of canine parvovirus. J. Virol. **76:**4401–4411.
47. **Türler, H., and P. Beard.** 1985. Simian virus SV40 and polyomavirus: growth, titration, transformation and purification of viral components, p. 169–192. *In* B. W. J. Mahy (ed.), Virology: a practical approach. IRL Press, Oxford, United Kingdom.
48. **White, J., L. Johannes, F. Mallard, A. Girod, S. Grill, S. Reinsch, P. Keller, B. Tzschaschel, A. Echard, B. Goud, and E. H. K. Stelzer.** 1999. Rab6 coordinates a novel Golgi to endoplasmic reticulum retrograde transport pathway in live cells. J. Cell Biol. **147:**743–759.
49. **Wilcke, M., L. Johannes, T. Galli, V. Mayau, B. Goud, and J. Salamero.** 2000. Rab11 regulates the compartmentalisation of early endosomes required for efficient transport from early endosomes to the trans-Golgi network. J. Cell Biol. **151:**1207–1220.
50. **Yamashiro, D. J., and F. R. Maxfield.** 1987. Acidification of morphologically distinct endosomes in mutant and wild-type Chinese hamster ovary cells. J. Cell Biol. **105:**2723–2733.